

## Electron-Density Analysis at 155 K by X-ray and Neutron Diffraction of *meso*-2,3-Bis(dimethylamino)butanedinitrile, C<sub>8</sub>H<sub>14</sub>N<sub>4</sub>

BY A. PARFONRY, J.-P. DECLERCQ, B. TINANT AND M. VAN MEERSSCHE

*Laboratoire de chimie physique et de cristallographie, Université Catholique de Louvain, 1 place Louis Pasteur,  
1348 Louvain la Neuve, Belgium*

AND P. SCHWEISS\*

*Laboratoire Léon Brillouin, Centre d'études nucléaires de Saclay, 91191 Gif sur Yvette, France*

(Received 7 October 1987; accepted 4 March 1988)

### Abstract

$M_r = 166.23$ , monoclinic,  $P2_1/a$ ,  $a = 10.417(2)$ ,  $b = 6.213(1)$ ,  $c = 7.918(1)$  Å,  $\beta = 110.42(2)^\circ$ ,  $V = 480.3(2)$  Å<sup>3</sup>,  $Z = 2$ ,  $D_x = 1.15$  g cm<sup>-3</sup>,  $T = 155$  K. X-ray: Mo  $K\alpha$ ,  $\lambda = 0.71069$  Å,  $\mu = 0.81$  cm<sup>-1</sup>,  $F(000) = 180$ ,  $R = 0.027$  for 1641 observed reflections. Neutron:  $\lambda = 0.8318$  Å,  $\mu = 1.93$  cm<sup>-1</sup>,  $R = 0.036$  for 786 observed reflections. Deformation density maps obtained by  $X-X$ ,  $X-N$  and dynamic techniques are compared. The results are quite similar, but a very unusual density in the central bond could only be interpreted on the basis of molecular disorder. The need to pay attention to such weak disorders, undiscernible at room temperature, is emphasized, as they can result in incorrect atomic positions and bond lengths.

### Introduction

This analysis continues our investigation on charge-density determination in dehydro dimers corresponding to the formula  $(R_1R_2R_3C-)_2$ . In previous work (Declercq, Tinant, Parfonry, Van Meerssche, Legrand & Lehmann, 1983), deformation density maps have been obtained for 1,1,2,2-ethanetetracarbonitrile at 158 K. In that case, two of the substituents ( $R_1$ ,  $R_2$ ) were electron-acceptor groups  $[-CN]$ , whereas in the present case, one of these groups has been replaced by an electron-donor substituent  $[-N(CH_3)_2]$ .

In addition to the low-temperature study mentioned above, we determined the X-ray crystal structures at room temperature of 24 molecules of the same general formula (Parfonry, Tinant, Declercq & Van Meerssche, 1987, and references cited therein). In some of these molecules, a stretched central bond length up to 1.61 Å was observed, and some stretching occurred in 1,1,2,2-ethanetetracarbonitrile, with a length of 1.561 Å. On the other hand, some molecules like the present one

(Parfonry, Tinant, Declercq & Van Meerssche, 1983) have a more normal central distance (1.543 Å). The aim is thus to analyse the effects of substitution on the electron density, mainly in the region of the central bond.

### Experimental

#### *X-ray*

Crystal size:  $1.5 \times 10^{-2}$  mm<sup>3</sup>. Cell parameters from the centring of 30 reflections in the range  $5 \leq 2\theta \leq 35^\circ$ . Syntex  $P2_1$  diffractometer, graphite-monochromatized Mo  $K\alpha$  radiation. Intensities were measured in the  $\theta/2\theta$  scan mode over the range  $2\theta(\alpha_1) - 1.8^\circ$  to  $2\theta(\alpha_2) + 1.8^\circ$  and recorded as 248 steps. The profile analysis of Blessing, Coppens & Becker (1972) was used to decide which parts of these steps were considered as peak and as background. For  $2\theta \leq 55^\circ$ , the complete sphere of reflections (four equivalents) was collected. In the range  $55 < 2\theta < 95^\circ$ , 1019 independent reflections were selected according to their intensity computed from the known structure at room temperature. For each of these high-order reflections, two symmetry equivalent reflections were collected. The total number of reflections was 6226 of which 2079 were independent, with  $R_{int} = 0.017$ . Of these, 1641 were observed with  $I \geq 2.5\sigma(I)$ . Absorption was very weak and not corrected: transmission factors computed between 0.972 and 0.984. Standard reflection (112) checked every 50 reflections: no significant deviation.  $hkl$  range:  $h -19-16$ ,  $k -11-11$ ,  $l -14-14$ .

#### *Neutron*

Crystal obtained by slow evaporation from 1:1 benzene-ethyl acetate. Crystal size: 11.5 mm<sup>3</sup>. Data collected with the 5C2 four-circle diffractometer at the Orphee reactor, Centre d'études nucléaires de Saclay.  $\theta-2\theta$  scan mode. For  $2\theta \leq 50^\circ$ , one complete asymmetric unit was collected. In the range  $50 < 2\theta < 75^\circ$ , we selected 605 independent reflections in a way similar

\* On leave from Kernforschungszentrum Karlsruhe, INFP, D-7500 Karlsruhe, and Institut für Mineralogie der Universität Marburg, D-3550 Marburg, Federal Republic of Germany.

to that explained for the X-ray study. The total scan width varied from 1.8 to 3.5° as a function of  $2\theta$ . A profile analysis was applied to the 1263 reflections collected. 1108 of these are independent,  $R_{\text{int}} = 0.006$ , and 786 were observed [ $I \geq 2.5\sigma(I)$ ]. Absorption was corrected dividing the volume of the crystal into 384 elements: transmission factors between 0.577 and 0.747. Standard reflection (631) checked every 50 reflections: no significant deviation.  $hkl$  range:  $h$  0–13,  $k$  0–9,  $l$  –11–10.

### Refinements

With the aim of producing electron-density deformation maps, three different kinds of refinements were performed, starting from the known parameters determined at room temperature (Parfonry *et al.*, 1983). The results allow a comparison of the deformation electron density obtained by the various techniques ( $X$ - $X$ ,  $X$ - $N$  and dynamic electron density). In all the refinements, the weighting schemes were adjusted to give a good analysis of  $\sum w\Delta^2$  as a function of the magnitude of  $F_{\text{obs}}$ .

#### Neutron refinement ( $N$ )

An extinction correction, following the formalism of Becker & Coppens (1974*a,b*, 1975) was tentatively applied, using the programme *RADIEL* (Coppens, Guru Row, Leung, Stevens, Becker & Yang, 1979). It was finally discarded, the most severe correction being higher than 0.99. Anisotropic least-squares refinement (*SHELX76*, Sheldrick, 1976) using  $F$ . 118 variables refined.  $w = 1/(\sigma^2 + 0.0001F^2)$ ,  $R = 0.036$ ,  $wR = 0.028$ ,  $S = 1.22$ . Final maximum shift to e.s.d. = 0.09. Scattering lengths from Koester & Rauch (1981).

#### X-ray multipolar refinement ( $X_1$ )

This kind of refinement was described in detail by Hansen & Coppens (1978), and the computations were performed using the programme *MOLLY* of the same authors. In this technique, the refined model has to represent the total electron density, including the modifications of the spherical atoms due to the chemical bonds. The model for each atom will thus consist of an aspherical density distribution obtained by the superposition of one monopole, three dipoles ... nine hexadecapoles, in addition to an undisturbed core density.

1641 observed independent reflections included. Refinement based on  $F$ . Atomic scattering factors from Fukamachi (1971) for C and N, and from Stewart, Davidson & Simpson (1965) for H. Thermal parameters of H atoms fixed at modified neutron values (see *Discussion*). Various extinction models described by Becker & Coppens (1974*a,b*, 1975) were tested, leading to the best results for an isotropic correction of type I with a Lorentzian distribution. A mosaic spread

distribution of 88'' was estimated, giving a factor of 0.95 for the largest correction applied to  $F^2$ . In order to minimize the number of refined parameters, local symmetries were imposed to the multipole functions: two mirror planes ( $mm$ ) for the cyano group C(2)–N(3); for N(4), a mirror plane through C(1), N(4) and the midpoint of C(5)–C(6); for C(5), a mirror plane through N(4), C(5) and H(5*a*). The populations and the deformation functions of the poles associated with C(6) were made identical to those of C(5). For H atoms, only one dipole in the direction of the C–H bond was refined. 166 variables.  $w = 1/(\sigma^2)$ ,  $R = 0.027$ ,  $wR = 0.013$ ,  $S = 1.81$ . Final maximum shift to e.s.d. on positional and thermal parameters: 0.15 for C.N and 0.4 for H. Scale factor: 0.833 (4).

#### X-ray high-order refinement ( $X_2$ )

558 observed independent reflections in the range  $0.70 \leq \sin\theta/\lambda \leq 1.04 \text{ \AA}^{-1}$ . Extinction correction kept at values obtained from the previous multipolar refinement. Anisotropic least-squares refinement (*SHELX76*, Sheldrick, 1976) using  $F$ . H atoms fixed at modified neutron values. 55 variables.  $w = 1/(\sigma^2 + 0.00007F^2)$ ,  $R = 0.052$ ,  $wR = 0.042$ ,  $S = 1.23$ . Final maximum shift to e.s.d. = 0.14. Scale factor: 0.784 (13). Atomic scattering factors from *International Tables for X-ray Crystallography* (1974).

### Discussion

Fig. 1 is a stereoscopic view of the molecule, showing the numbering of the atoms; the atomic parameters are given in Table 1.\* As can be seen from this table, the anisotropic thermal parameters show systematic discrepancies between the three refinements. Comparing the two X-ray results first, the values from the multipole refinement ( $X_1$ ) are higher by a mean factor of 1.05

\* Lists of structure factors have been deposited with the British Library Document Supply Centre as Supplementary Publication No. SUP 44823 (15 pp.). Copies may be obtained through The Executive Secretary, International Union of Crystallography, 5 Abbey Square, Chester CH1 2HU, England.

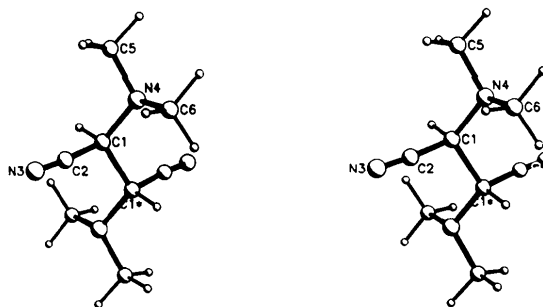


Fig. 1. Stereoscopic view of the molecule and numbering of the atoms (*PLUTO*; Motherwell & Clegg, 1978).

Table 1. *Positional ( $\times 10^4$ ) and thermal parameters ( $\text{\AA}^2 \times 10^4$ )* $X_1$  = multipolar refinement,  $X_2$  = high-order refinement.

	<i>x</i>	<i>y</i>	<i>z</i>	$U_{11}$	$U_{22}$	$U_{33}$	$U_{12}$	$U_{23}$	$U_{13}$
C(1)									
$X_1$	-331 (2)	812 (1)	5470 (1)	179 (3)	144 (3)	185 (3)	20 (3)	0 (3)	63 (3)
$X_2$	-330 (2)	806 (2)	5474 (2)	171 (5)	134 (5)	167 (5)	9 (3)	-3 (3)	66 (4)
<i>N</i>	-330 (2)	810 (2)	5473 (2)	192 (7)	149 (6)	178 (6)	9 (6)	-6 (6)	67 (5)
C(2)									
$X_1$	-1183 (1)	-421 (1)	6310 (1)	217 (3)	202 (3)	237 (3)	-35 (2)	-32 (2)	111 (3)
$X_2$	-1184 (2)	-412 (2)	6303 (2)	201 (6)	191 (6)	232 (6)	-33 (4)	-31 (4)	106 (4)
<i>N</i>	-1191 (2)	-416 (2)	6300 (2)	216 (7)	203 (7)	264 (7)	-35 (6)	-40 (6)	120 (6)
N(3)									
$X_1$	-1817 (1)	-1275 (1)	7053 (1)	304 (3)	286 (3)	323 (4)	-72 (2)	-27 (2)	187 (4)
$X_2$	-1819 (2)	-1268 (3)	7048 (3)	297 (8)	275 (7)	319 (8)	-87 (5)	-33 (5)	184 (6)
<i>N</i>	-1824 (1)	-1266 (2)	7037 (2)	304 (6)	313 (7)	353 (6)	-85 (6)	-31 (5)	202 (5)
N(4)									
$X_1$	694 (1)	2165 (1)	6745 (1)	220 (3)	172 (2)	205 (3)	-25 (3)	-45 (2)	75 (2)
$X_2$	686 (2)	2171 (2)	6742 (2)	200 (6)	164 (5)	182 (5)	-23 (4)	-44 (4)	63 (4)
<i>N</i>	678 (1)	2158 (2)	6748 (1)	198 (5)	177 (4)	214 (5)	-29 (5)	-46 (5)	77 (4)
C(5)									
$X_1$	61 (1)	4026 (1)	7268 (1)	329 (3)	211 (3)	330 (3)	2 (2)	-76 (2)	132 (3)
$X_2$	63 (2)	4040 (3)	7269 (3)	325 (8)	191 (7)	332 (9)	0 (5)	-81 (5)	134 (6)
<i>N</i>	52 (2)	4014 (3)	7277 (2)	340 (9)	221 (8)	374 (9)	-9 (8)	-100 (8)	150 (8)
C(6)									
$X_1$	1596 (1)	1043 (1)	8333 (1)	259 (3)	319 (3)	227 (3)	27 (2)	-38 (2)	34 (2)
$X_2$	1597 (2)	1044 (4)	8324 (3)	246 (7)	300 (8)	214 (7)	25 (5)	-51 (5)	17 (5)
<i>N</i>	1576 (2)	1026 (3)	8330 (2)	268 (9)	331 (10)	240 (8)	29 (7)	-49 (7)	26 (7)
H(1)									
$X_1$	-994 (13)	1773 (20)	4494 (18)						
<i>N</i>	-1034 (3)	1872 (6)	4441 (4)	310 (16)	296 (17)	Fixed at modified <i>N</i> values 362 (16)	75 (14)	37 (13)	75 (13)
H(5a)									
$X_1$	-521 (10)	3586 (19)	8081 (15)						
<i>N</i>	-549 (5)	3582 (7)	8124 (6)	708 (29)	564 (25)	753 (27)	50 (25)	-95 (24)	497 (24)
H(5b)									
$X_1$	847 (13)	5084 (17)	7992 (16)						
<i>N</i>	861 (5)	5136 (7)	8037 (6)	636 (28)	371 (22)	733 (28)	-113 (20)	-255 (21)	205 (23)
H(5c)									
$X_1$	-602 (12)	4799 (15)	6126 (18)						
<i>N</i>	-618 (5)	4867 (7)	6099 (6)	654 (28)	371 (22)	595 (26)	187 (20)	17 (19)	126 (22)
H(6a)									
$X_1$	2101 (9)	-215 (18)	7982 (15)						
<i>N</i>	2118 (4)	-288 (7)	7952 (5)	480 (22)	490 (23)	500 (22)	191 (20)	-68 (19)	7 (18)
H(6b)									
$X_1$	2307 (11)	2121 (19)	9099 (13)						
<i>N</i>	2338 (4)	2162 (8)	9154 (5)	476 (22)	621 (27)	511 (23)	-94 (21)	-210 (21)	-77 (18)
H(6c)									
$X_1$	1072 (10)	460 (16)	9152 (15)						
<i>N</i>	1025 (5)	388 (9)	9179 (6)	572 (25)	807 (33)	444 (20)	65 (25)	217 (22)	202 (20)

than those from the high-order refinement ( $X_2$ ); this difference can be attributed to high correlations in the refinement calculations between the temperature factors, the scale factor and the multipolar population and extension parameters. The largest difference occurs between the neutron ( $N$ ) and the high-order ( $X_2$ ) results:  $\langle U(X_2) \rangle / \langle U(N) \rangle = 0.91$ . In principle, the opposite effect should be expected, like, for example in tetracyanoethylene (Becker, Coppens & Ross, 1973) since the neutron results are not biased by the electron-density distribution. However, similar situations are not unusual and have been explained as resulting from a higher temperature for the neutron data collection (Coppens & Vos, 1971). Another interpretation considering differences in the thermal diffuse scattering of the neutron and X-ray data was suggested by Coppens (1978). The latter explanation seems more appropriate since the temperature was carefully adjusted in both experiments. As was pointed out by Hirshfeld & Hope (1980), scan truncation losses in the high-order reflections can also be responsible for discrepancies between temperature factors. In the present case, however, this interpretation does not seem to be applicable because it

would imply a systematic underestimation of the reflections concerned; this was not observed. Moreover, such a correction would increase the X-ray high-order  $F_o$  values and decrease the corresponding temperature factors even further. The best remedy is to multiply the neutron thermal parameters by an empirical factor (0.91 in the present case) when neutron results have to be combined directly with X-ray results. Such 'corrected' values have been reported in the *Refinements* section as 'modified neutron values'. Bond distances and angles from the three refinements are compared in Table 2.

#### Density deformation

Chronologically, the X-ray data were collected before the neutron data, and the first deformation maps produced were  $X$ - $X$  maps resulting from the high-order refinement and dynamic maps resulting from the multipolar refinements. These initial maps were very similar to the  $X$ - $X$  and dynamic maps produced later using the neutron parameters for the H atoms and the X-ray parameters for C and N atoms (high-order

Table 2. Bond distances (Å) and angles (°)

	N	X <sub>1</sub>	X <sub>2</sub>
C(1)–C(1)*	1.551 (3)	1.551 (1)	1.549 (3)
C(1)–C(2)	1.491 (2)	1.493 (1)	1.484 (3)
C(2)–N(3)	1.150 (2)	1.155 (1)	1.158 (3)
C(1)–N(4)	1.443 (2)	1.454 (1)	1.451 (2)
N(4)–C(5)	1.456 (2)	1.461 (1)	1.460 (3)
N(4)–C(6)	1.456 (2)	1.458 (1)	1.460 (2)
C(1)–H(1)	1.106 (4)	1.029 (11)	
C(5)–H(5)	1.099 (4)	1.063 (13)	
C(5)–H(5')	1.097 (5)	1.051 (11)	
C(5)–H(5'')	1.088 (5)	1.044 (11)	
C(6)–H(6)	1.092 (5)	1.033 (12)	
C(6)–H(6')	1.092 (5)	1.025 (11)	
C(6)–H(6'')	1.099 (5)	1.047 (13)	
C(1)*–C(1)–C(2)	108.5 (1)	108.2 (1)	108.7 (2)
C(1)*–C(1)–N(4)	112.2 (1)	111.6 (1)	111.9 (2)
C(2)–C(1)–N(4)	113.1 (1)	113.2 (1)	113.4 (1)
C(1)–C(2)–N(3)	175.3 (2)	175.4 (1)	175.4 (2)
C(1)–N(4)–C(5)	111.8 (1)	111.1 (1)	111.9 (1)
C(1)–N(4)–C(6)	114.4 (1)	114.8 (1)	114.4 (1)
C(5)–N(4)–C(6)	110.7 (1)	110.7 (1)	110.9 (2)
C(1)*–C(1)–H(1)	108.8 (2)	108.2 (8)	
C(2)–C(1)–H(1)	106.5 (2)	106.6 (8)	
N(4)–C(1)–H(1)	107.7 (2)	108.9 (7)	
N(4)–C(5)–H(5)	113.0 (3)	112.2 (6)	
N(4)–C(5)–H(5')	109.0 (3)	107.9 (7)	
N(4)–C(5)–H(5'')	110.9 (3)	110.3 (7)	
H(5)–C(5)–H(5')	108.2 (4)	109.3 (9)	
H(5)–C(5)–H(5'')	108.1 (4)	107.4 (9)	
H(5')–C(5)–H(5'')	107.5 (4)	109.8 (8)	
N(4)–C(6)–H(6)	111.3 (3)	111.4 (6)	
N(4)–C(6)–H(6')	108.5 (3)	108.2 (6)	
N(4)–C(6)–H(6'')	112.6 (3)	112.4 (5)	
H(6)–C(6)–H(6')	108.0 (4)	108.8 (8)	
H(6)–C(6)–H(6'')	109.2 (4)	109.2 (9)	
H(6')–C(6)–H(6'')	107.1 (4)	106.5 (9)	

parameters for  $X$ – $X$  and multipolar parameters for dynamic maps). Some characteristic sections of the later maps are shown in Figs. 2 ( $X$ – $X$ ) and 3 (dynamic).  $X$ – $X$  maps produced with data limited to  $\sin\theta/\lambda = 0.65 \text{ \AA}^{-1}$  are presented with a contour interval of  $0.1 e \text{ \AA}^{-3}$ , and dynamic maps, including all the observed data, with a finer contour interval of  $0.05 e \text{ \AA}^{-3}$ . It can be seen that clean and comparable results are obtained nearly everywhere: the electron densities are about  $0.4 e \text{ \AA}^{-3}$  in the central bond,  $0.3 e \text{ \AA}^{-3}$  in  $C(1)$ – $N(4)$  and  $C(1)$ – $C(2)$ , and  $0.7 e \text{ \AA}^{-3}$  in the triple  $C(2)$ – $N(3)$  bond, with cylindrical distributions in the last three bonds. Discrepancies occur only in the vicinity of the nuclear positions, where it is well known that the experimental difference maps are unreliable and very dependent on the scale factor. Fig. 4 shows the central bond computed with the two techniques in the  $H(1)C(1)C(1)^*$  plane. It presents a very unusual density distribution which could not be distinguished even in the  $N(4)C(1)C(1)^*$  plane showing the same bond in a different orientation. The density in this central bond seems to be far from cylindrical. Error maps were computed according to Rees (1976, 1978); estimated standard deviations of only  $0.05 e \text{ \AA}^{-3}$  appear in that region. As such peculiarities occur only in a very limited part of the unit cell, it seemed quite improbable that they could be attributed to experimental error and it was decided to collect neutron data mainly to provide accurate H-atom parameters, especially for  $H(1)$ , which is certainly strongly associated with this abnormal density.

The  $X$ – $N$  maps were obtained by subtracting from the  $X$ -ray data limited to  $\sin\theta/\lambda = 0.65 \text{ \AA}^{-1}$ ; the corresponding structure factors computed with the 'modified neutron values'. The resulting maps are comparable to the previous  $X$ – $X$  and dynamic maps,

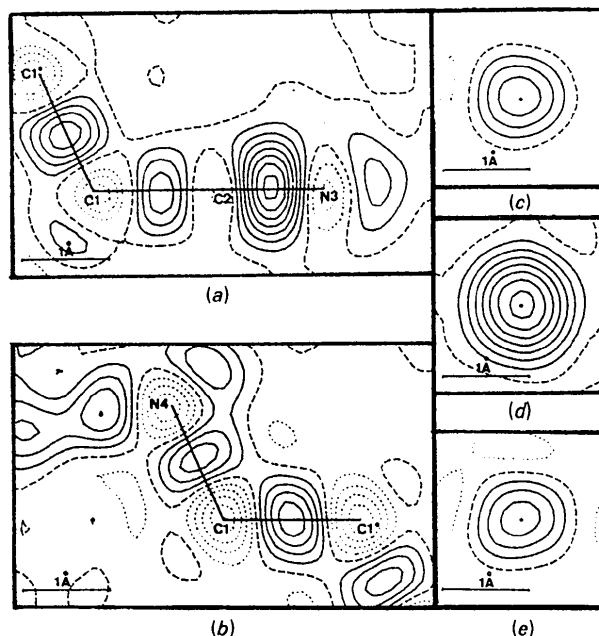


Fig. 2.  $X$ – $X$  deformation maps. Contours at  $0.1 e \text{ \AA}^{-3}$  (— positive, --- zero, ... negative). Sections in the plane  $C(1)C(1)^*N(3)$  (a); in the plane  $C(1)C(1)^*N(4)$  (b); perpendicular to the bonds  $C(1)$ – $C(2)$  (c),  $C(2)$ – $N(3)$  (d), and  $C(1)$ – $N(4)$  (e).

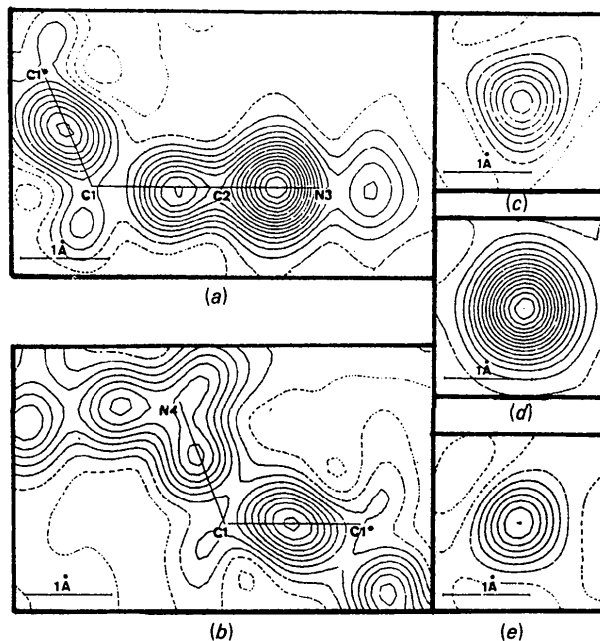


Fig. 3. Dynamic deformation maps. Contours at  $0.05 e \text{ \AA}^{-3}$ . Sections as in Fig. 2.

and Fig. 5 clearly shows that the neutron data did not solve the particular problem of the central bond.

On the other hand, the neutron data by themselves allow a difference Fourier map to be computed in the same

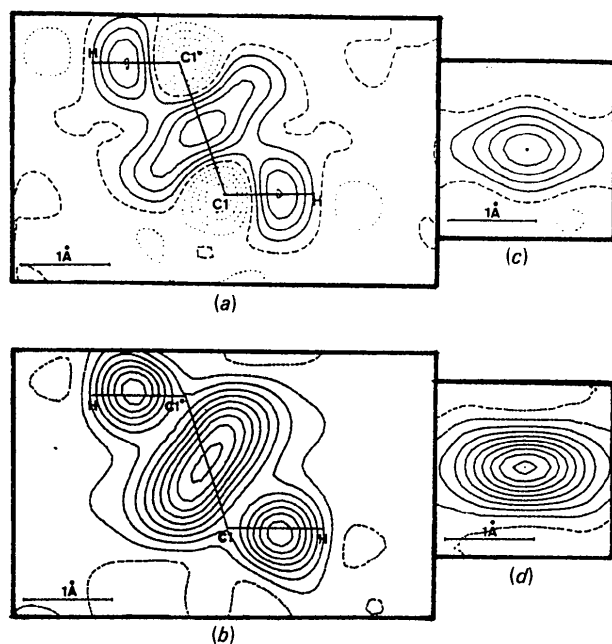


Fig. 4. The central bond in the plane  $C(1)C(1)^*H$ :  $X-X$  (a); dynamic (b). Sections perpendicular to the same bond:  $X-X$  (c); dynamic (d). Contours as in Figs. 2 and 3.

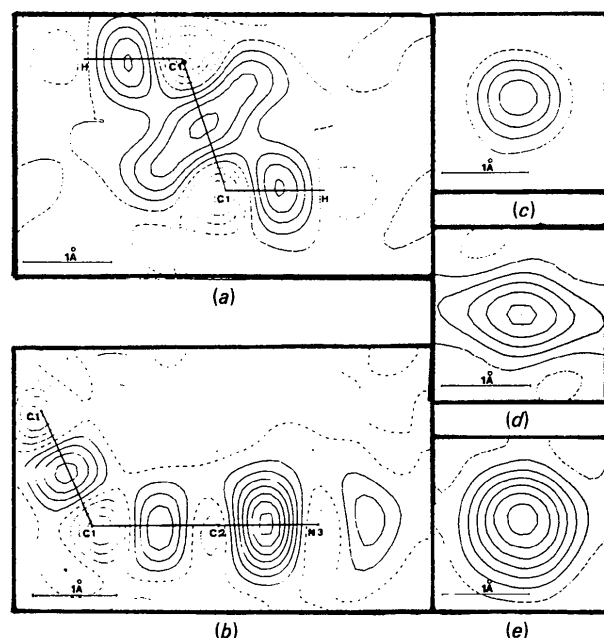


Fig. 5.  $X-N$  deformation maps. Contours at  $0.1 e \text{ \AA}^{-3}$ . The central bond in the plane  $C(1)C(1)^*H$  (a); section in the plane  $C(1)C(1)^*N(3)$  (b); sections perpendicular to the bonds  $C(1)-C(2)$  (c),  $C(1)-C(1)^*$  (d), and  $C(2)-N(3)$  (e).

region (Fig. 6). One can expect, if the special deformation observed in X-ray maps is purely electronic that a neutron difference map will be very flat, as there would be no nuclei involved in that deformation. This is not at all the case and may suggest an orientational disorder of the molecule: the two most important positive peaks could represent the second position of the central C atoms, while the two negative regions could correspond to the H atoms with negative scattering lengths. To accept such a disordered model, it should be possible to build a molecular model showing the two orientations in which all the atoms could be nearly superimposed, except  $H-C-C-H$  in the central bond. Such a model is shown in Fig. 7. The coordinates of this 'inverted' molecule and the distances to the corresponding atom in the main molecule are given in Table 3. This table is limited to the rigid part of the molecule because no information is available about the torsion angles defining the methyl groups in the disordered molecule. For the atoms  $C(2)$ ,  $N(3)$  and  $N(4)$ , the maximum distance is  $0.2 \text{ \AA}$  and it is not surprising that nothing appears if the occupation factor of this second molecule is very weak. Another convincing result is presented in Fig. 8, which shows the residual density in the plane of these atoms, obtained by subtracting the experimental density from the density of

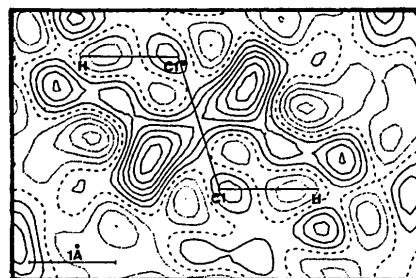


Fig. 6. Difference Fourier map using neutron data, in the plane  $C(1)C(1)^*H$ . Contours at  $0.1 \text{ fermi \AA}^{-3}$ .

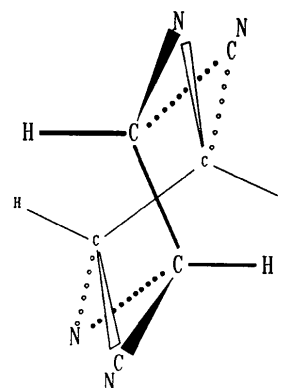


Fig. 7. Model suggesting a disorder compatible with the observed densities: all the atoms are nearly superimposed, except in the central bond.

Table 3. Coordinates of the rigid part of the inverted molecule ( $\times 10^4$ ) and distances to the main molecule (Å)

	x	y	z	d
C(1)	186	67	6036	0.73
C(2)	-1020	-662	6486	0.24
N(3)	-1930	-1113	6921	0.15
N(4)	662	2181	6731	0.02
H(1)	1020	-1088	6884	2.91

the multipolar model. Such a map clearly shows that the multipolar refinement was not able to account for the electron density in this region of the molecule, and this is a further argument for disorder. Of course this map was computed at the end of the multipolar refinement, and could have been the first hint for disorder. However, as the map contained only one residual large peak the idea of such a peculiar disorder was not considered at that time. The occupation factor of the second orientation is so weak that attempts to obtain the value of this factor from X-ray constrained refinements were unsuccessful. Such a weak disorder is not unusual and has been reported for example in tetracyanoethylene (Drück & Guth, 1982).

### Conclusion

Our first aim was to compare the density in the central bond with that observed in 1,1,2,2-ethanetetracarbonitrile to get some information about the substituent effects. As orientational disorder is the most likely explanation of the deformation maps observed here, comparison between the two compounds is now obsolete.

One must be very careful when interpreting results of X-ray diffraction data, as it is well known that a weak

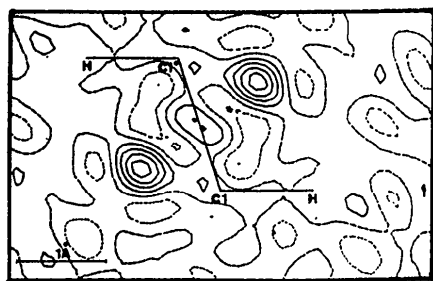


Fig. 8. Residual map. Contours at  $0.05 \text{ e} \cdot \text{Å}^{-3}$ . Section in the plane  $C(1)C(1)^*H$ .

unresolved disorder will usually give apparently shortened bond lengths. This could also explain some of the discrepancies between the values in Table 2. Such a disorder can only be distinguished after careful measurements and interpretations of low-temperature data and can be harmful, for example, if one has to compare bond lengths in a series of molecules found in the literature.

AP, JPD, BT and MVM thank the Service de la Programmation de la Politique Scientifique et le Fonds de Développement Scientifique de l'Université Catholique de Louvain for financial support and the Laboratory of Organic Chemistry of this University (Professor H. G. Viehe) for providing the compound.

### References

- BECKER, P. J. & COPPENS, P. (1974a). *Acta Cryst.* **A30**, 129–147.  
 BECKER, P. J. & COPPENS, P. (1974b). *Acta Cryst.* **A30**, 148–153.  
 BECKER, P. J. & COPPENS, P. (1975). *Acta Cryst.* **A31**, 417–425.  
 BECKER, P. J., COPPENS, P. & ROSS, F. K. (1973). *J. Am. Chem. Soc.* **95**, 7604–7609.  
 BLESSING, R. H., COPPENS, P. & BECKER, P. J. (1972). *J. Appl. Cryst.* **7**, 488–492.  
 COPPENS, P. (1978). *Top. Curr. Phys.* **6**, 71–111.  
 COPPENS, P., GURU ROW, T. N., LEUNG, P., STEVENS, E. D., BECKER, P. J. & YANG, Y. W. (1979). *Acta Cryst.* **A35**, 63–72.  
 COPPENS, P. & VOS, A. (1971). *Acta Cryst.* **B27**, 146–158.  
 DECLERCQ, J.-P., TINANT, B., PARFONRY, A., VAN MEERSSCHE, M., LEGRAND, E. & LEHMANN, M. S. (1983). *Acta Cryst.* **C39**, 1401–1405.  
 DRÜCK, U. & GUTH, H. (1982). *Z. Kristallogr.* **161**, 103–110.  
 FUKAMACHI, T. (1971). Tech. Rep. Inst. Solid State Phys. Univ. Tokyo, Ser. B, No. 12. Univ. of Tokyo, Japan.  
 HANSEN, N. K. & COPPENS, P. (1978). *Acta Cryst.* **A34**, 909–921.  
 HIRSHFELD, F. L. & HOPE, H. (1980). *Acta Cryst.* **B36**, 406–415.  
*International Tables for X-ray Crystallography* (1974). Vol. IV. Birmingham: Kynoch Press. (Present distributor Kluwer Academic Publishers, Dordrecht.)  
 KOESTER, L. & RAUCH, H. (1981). *Summary of Neutron Scattering Lengths*. IAEA contract 2517/RB. Vienna: IAEA.  
 MOTHERWELL, S. & CLEGG, W. (1978). *PLUTO*. Univ. of Cambridge, England.  
 PARFONRY, A., TINANT, B., DECLERCQ, J.-P. & VAN MEERSSCHE, M. (1983). *Bull. Soc. Chim. Belg.* **92**, 437–443.  
 PARFONRY, A., TINANT, B., DECLERCQ, J.-P. & VAN MEERSSCHE, M. (1987). *Bull. Soc. Chim. Belg.* **96**, 89–95.  
 REES, B. (1976). *Acta Cryst.* **A32**, 483–488.  
 REES, B. (1978). *Acta Cryst.* **A34**, 254–256.  
 SHELDRICK, G. M. (1976). *SHELX76*. Program for crystal structure determination. Univ. of Cambridge, England.  
 STEWART, R. F., DAVIDSON, E. R. & SIMPSON, W. T. (1965). *J. Chem. Phys.* **42**, 3175–3187.